Journal of Applied Polymer Science

Enhanced nonisothermal and isothermal cold crystallization kinetics of biodegradable poly(L-lactide) by trisilanolisobutyl-polyhedral oligomeric silsesquioxanes in their nanocomposites

Lu Tang, Zhaobin Qiu
State Key Laboratory of Chemical Resource Engineering, MOE Key Laboratory of Carbon Fiber and Functional Polymers, Beijing University of Chemical Technology, Beijing, 100029, China
Correspondence to: Z. Qiu (E-mail: qiuzb@mail.buct.edu.cn)

ABSTRACT: In this work, the nonisothermal and isothermal cold crystallization behaviors of poly(L-lactide) (PLLA)/trisilanolisobutyl-polyhedral oligomeric silsesquioxanes (tsib-POSS) nanocomposites with low tsib-POSS contents were fully investigated. For all the samples, the variations of heating rate and the tsib-POSS loading may influence the nonisothermal cold crystallization of PLLA. During the nonisothermal crystallization kinetics study, the Ozawa equation failed to fit the nonisothermal crystallization process of PLLA, while the Tobin equation could fit it well. For the isothermal crystallization kinetics study, the crystallization rates of all the samples increased with increasing crystallization temperature. The cold crystallization activation energy of PLLA was increased with 1 wt % tsib-POSS. Moreover, the addition of tsib-POSS and the increment of tsib-POSS loading could increase the crystallization rate of PLLA, indicating the nucleating agent effect of tsib-POSS. However, the crystallization mechanism and crystal structure of PLLA remained unchanged in the nanocomposites. © 2016 Wiley Periodicals, Inc. J. Appl. Polym. Sci. **2016**, *133*, 43896.

KEYWORDS: biodegradable; crystallization; differential scanning calorimetry (DSC)

Received 25 January 2016; accepted 5 May 2016
DOI: 10.1002/app.43896

INTRODUCTION

Considering the shortage of petroleum resource and the environmental pollution caused by nondegradable plastics, polymers derived from renewable resources stand out as a potential replacement, among which poly(L-lactide) (PLLA) is the most promising one because of its attractive mechanical properties, transparency, biodegradability and biocompatibility.[1–3] However, the slow crystallization rate of PLLA has limited its wider use from a practical viewpoint. The compounding of nanofiller with PLLA is an efficient way to enhance the crystallization rate of PLLA. Till now, a number of nanofillers have been used to fabricate PLLA-based nanocomposites.[4–16] The results indicated that the crystallization process of PLLA was obviously accelerated by only a small amount of nanofillers, thus promoting the practical application fields of PLLA.

Polyhedral oligomeric silsesquioxanes (POSS), a kind of inorganic–organic nanofiller with core–shell structure, has attracted continuous interests in the past few decades; moreover, many researches have been performed to study the preparation, physical properties, and further application of different kinds of POSS.[17–21] Unlike the commonly used POSS with formula $R_8Si_8O_{12}$, trisilanolisobutyl-polyhedral oligomeric silsesquioxanes (tsib-POSS) has an open cage structure with formula $R_7Si_7O_{12}H_3$, where R is isobutyl. With the existence of hydroxyl and isobutyl end groups, the amphiphilic tsib-POSS was studied and used at the air/water interface.[22–24] Moreover, the rigid nature of the inorganic core of tsib-POSS was also utilized to increase the thermal stability of polymer matrix.[25–27] However, to the best of our knowledge, the biodegradable polymer/tsib-POSS nanocomposites or the nucleation agent effect of tsib-POSS particles has not been fully studied.[28]

During the study of semicrystalline polymer and polymer nanocomposites, the crystallization kinetics should be fully discussed for both the academical investigation and the industrial processing method design. It is noticeable that the crystallization process may happen not only when the samples are cooled from the melt state (which is named as melt crystallization) but also when the samples are heated from the amorphous state (which is called cold crystallization). The study of cold crystallization behavior is of vital importance and can broaden the processing ways of semicrystalline polymers from an application viewpoint; however, the cold crystallization behavior of semicrystalline polymers has not been fully investigated so far, compared with the melt crystallization behaviors.[9,11,15,29–31]

As the crystallization rate of PLLA is slow, PLLA is able to reach the fully amorphous state, making it possible to study the cold crystallization behavior of PLLA and its nanocomposites. In previous work, we prepared a PLLA/tsib-POSS nanocomposite at low tsib-POSS loading via a solution and casting method.[28] The results indicated that a small amount of tsib-POSS enhanced both the melt crystallization behavior and mechanical properties of PLLA by acting as both an efficient nucleating agent and a reinforcing filler in the PLLA matrix. In this work, we further investigated the addition of tsib-POSS and the change of tsib-POSS contents on the nonisothermal and isothermal cold crystallization behaviors of PLLA, for the purpose of broadening the potential application fields of PLLA.

EXPERIMENTAL

Materials

PLLA ($M_w = 1.58 \times 10^5$ g/mol) was kindly provided by Biomer company, Germany. The tsib-POSS sample was purchased from Changsha Passkey Instrument Co. Ltd, China, which was actually produced by Hybrid Plastics.

Sample Preparation

Two PLLA/tsib-POSS nanocomposites with the tsib-POSS contents of 0.5 and 1 wt % were prepared through a solution and casting method using chloroform as a solvent.[15] For simplicity, the nanocomposites were named as PLLA/tsib-POSS0.5 and PLLA/tsib-POSS1, respectively. Neat PLLA was treated with the same method.

Characterization

The cold crystallization behavior of the samples was investigated by a TA Instruments Q100 differential scanning calorimeter (DSC) under nitrogen purge. Indium standard was used for temperature calibration. The weights of all the samples were around 4–6 mg, and a fresh sample was used for each DSC run. For the nonisothermal cold crystallization study, the samples were first heated to 190 °C and held for 3 min to erase any previous thermal history (first heating process), cooled to 20 °C at 40 °C/min to ensure the samples reached the amorphous state, and followed by the second heating process to 190 °C again at various rates from 5 to 20 °C/min. The nonisothermal cold crystallization behavior was studied through the second heating process. To investigate the isothermal cold crystallization kinetics, the samples were cooled to 20 °C at 40 °C/min after annealing at 190 °C for 3 min. Then the samples were heated to the chosen isothermal crystallization temperature (T_c) at 60 °C/min and held till the isothermal crystallization process was complete. The chosen T_c values were from 90 to 105 °C.

Wide-angle X-ray diffraction (WAXD) patterns for the samples were obtained from a Rigaku D/Max 2500 VB2t/PC X-ray diffractometer at room temperature, and the scanning rate was 5°/min. All the samples were prepared by first pressing into thin films (~0.5 mm) at 190 °C on a hot stage for 3–5 min. The samples were then quenched into ice water, held for 1 h to fully reach the amorphous state, and quickly transferred into a vacuum oven at 90 °C for 3 days.

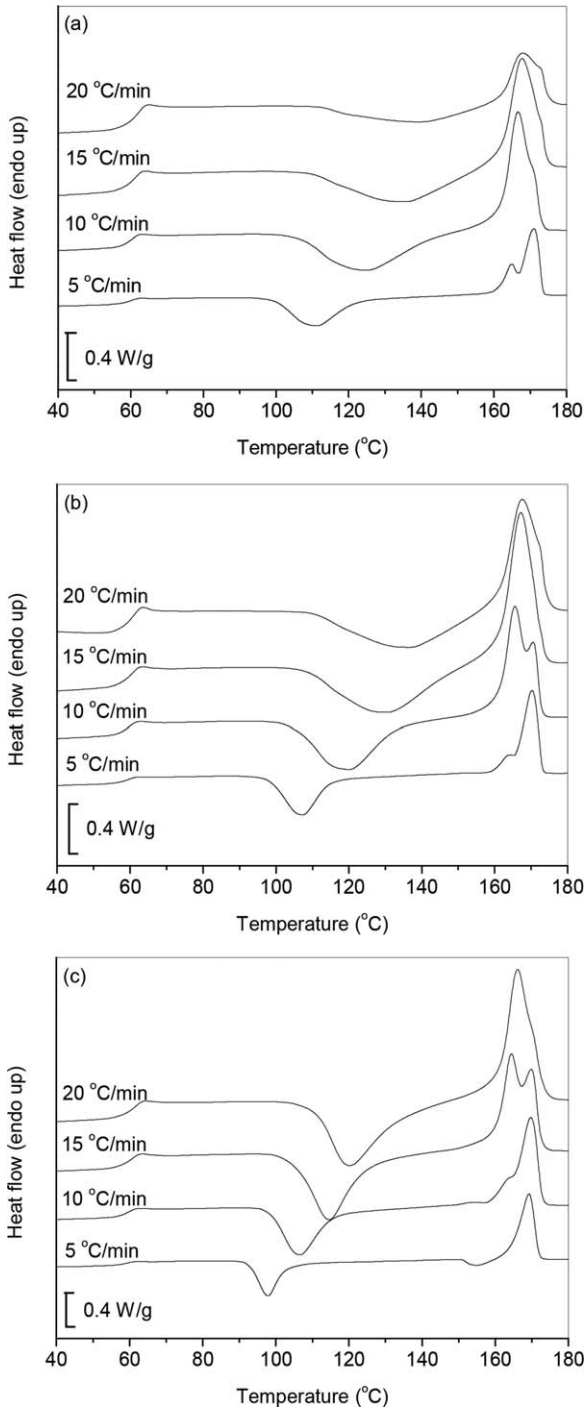

Figure 1. Nonisothermal cold crystallization behavior of (**a**) neat PLLA, (**b**) PLLA/tsib-POSS0.5, and (**c**) PLLA/tsib-POSS1 at indicated heating rates.

RESULTS AND DISCUSSION

Nonisothermal Cold Crystallization Behavior of Neat PLLA and its Nanocomposites

The nonisothermal cold crystallization behavior of PLLA and its nanocomposites is shown in Figure 1. Take neat PLLA as an example, the cold crystallization peak temperature (T_p) shifted upward from 111.1 to 139.5 °C when the heating rate increased

Table I. Summary of the Nonisothermal Cold Crystallization Behavior Parameters for Neat PLLA and its Nanocomposites

Samples	Φ (°C/min)	T_p[a] (°C)	ΔH_{ch}[b] (J/g)	$t_{1/2}$ (min)	CRC (min^{-1})	CRP ($°C^{-1}$)
Neat PLLA	5	111.1	48.6	4.50	0.530	0.0272
	10	125.0	46.2	2.99		
	15	135.7	30.6	2.17		
	20	139.5	12.3	1.58		
PLLA/tsib-POSS0.5	5	107.4	49.5	4.06	0.535	0.0279
	10	120.3	48.0	2.46		
	15	130.4	40.0	2.01		
	20	136.5	24.4	1.47		
PLLA/tsib-POSS1	5	98.0	41.3	2.28	0.739	0.0287
	10	106.6	43.8	1.64		
	15	114.6	45.4	1.37		
	20	120.0	39.4	1.14		

[a]The error is within ±0.1 °C.
[b]The error is within ±1 J/g.

from 5 to 20 °C/min; moreover, the crystallization exotherms became broader as well. Similar results were also found in the nanocomposites. All the detailed T_p values are listed in Table I.

It could also be concluded from Table I that increasing the tsib-POSS loading significantly decreased the T_p values of the nanocomposites. For instance, when the heating rate was 15 °C/min, the T_p values were 135.7, 130.4, and 114.6 °C for neat PLLA, PLLA/tsib-POSS0.5, and PLLA/tsib-POSS1, respectively. The decrease in T_p was only 5.3 °C between PLLA/tsib-POSS0.5 and neat PLLA, while the further addition of tsib-POSS from 0.5 to 1 wt % caused a significant 15.8 °C decrease in T_p between the two nanocomposites, indicating that the variation of T_p was mainly dependent on the tsib-POSS loading. The same trends were also found at other heating rates. In brief, T_p may shift to a lower temperature range with the decrease of heating rate and the increase of tsib-POSS loading.

Apart from the variation of T_p, it was also important to study the influences of heating rate and the tsib-POSS loading on the nonisothermal cold crystallization enthalpy (ΔH_{ch}) of PLLA in the nanocomposites. As shown in Table I, the ΔH_{ch} values of neat PLLA sharply dropped from 48.6 to 12.3 J/g with increasing heating rate from 5 to 20 °C/min, indicating that a heating rate of 20 °C/min was too fast for neat PLLA to adequately crystallize. Consequently, the crystallinity value of PLLA was reduced at a faster heating rate than at a slower heating rate. However, in the case of PLLA/tsib-POSS1, the ΔH_{ch} values slightly changed between 39.4 and 45.4 J/g when the heating rate varied from 5 to 20 °C/min. Moreover, at the heating rate of 20 °C/min, the ΔH_{ch} values for neat PLLA, PLLA/tsib-POSS0.5, and PLLA/tsib-POSS1 were 12.3, 24.4, and 39.4 J/g, respectively. Such result indicated that the increase of tsib-POSS loading increased the crystallinity of PLLA, thereby enhancing the nonisothermal cold crystallization of PLLA matrix at a fast heating rate. All the detailed ΔH_{ch} values are summarized in Table I. In conclusion, the nonisothermal cold crystallization behavior of neat PLLA and its nanocomposites was obviously affected by both heating rate and the tsib-POSS loading. Therefore, we may adjust the nonisothermal cold crystallization behavior of PLLA, depending on heating rate and the tsib-POSS loading.

As also shown in Figure 1, when the T_p value was below 100 °C, the DSC curve was characterized by a small exothermic peak just before the main melting peak, due to the formation of a disordered α′ form of PLLA. PLLA has α, β, γ, and α′-form crystals under different crystallization conditions.[32–37] The thermodynamically favored α-form crystal are produced from the cold or melt crystallization when the crystallization temperature is higher than 120 °C, while the kinetically favored α′-form crystal are formed at lower temperature, that is, below 100 °C.[34–37] In this work, when the cold crystallization occurred below 100 °C, the crystalline-phase transition from α' to α happened during the further heating process, leading to the appearance of a small exothermic peak prior to the final melting peak.[11,34] Moreover, when the T_p values of the samples were between 100 and 120 °C, two melting peaks or a shoulder peak beside a major melting peak were observed in the DSC heating traces, which were considered to be caused by the melting and recrystallization of the α form crystals.[11,37]

Figure 2 displays the plots of relative crystallinity versus crystallization time for all the samples during the nonisothermal cold crystallization process at a heating rate of 15 °C/min. As illustrated in Figure 2, it took shorter time for the nanocomposites to finish crystallization than for neat PLLA; moreover, the increased tsib-POSS loading may further accelerate the nonisothermal cold crystallization process. Similar trends were also observed at other heating rates. For brevity, they were not displayed here.

It was more directly to compare the time required to achieve 50% of the final crystallinity, that is, the half-time of cold crystallization ($t_{1/2}$) of the samples when mentioning about the nonisothermal cold crystallization rate. The $t_{1/2}$ values for all

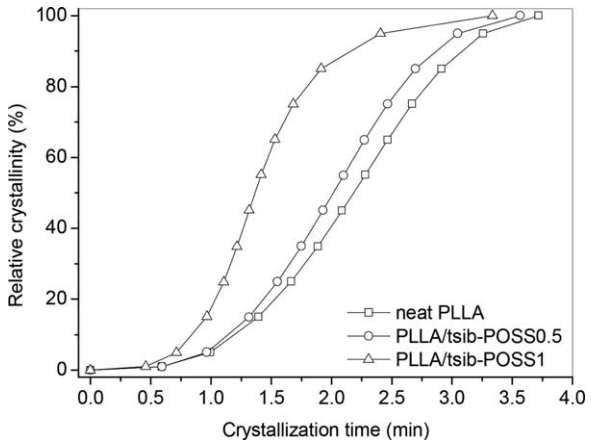

Figure 2. Plots of relative crystallinity versus crystallization time for neat PLLA and its nanocomposites at 15 °C/min.

the samples at various heating rates are also listed in Table I. With the increase of heating rate, the $t_{1/2}$ values decreased, indicating that the nonisothermal cold crystallization rate of PLLA was enhanced at higher heating rates. Moreover, at the same heating rate, neat PLLA presented a smaller $t_{1/2}$ value than its nanocomposites; furthermore, with the increase of tsib-POSS loading, the $t_{1/2}$ value decreased as well. In brief, tsib-POSS could enhance the nonisothermal cold crystallization behavior of PLLA.

The effect of tsib-POSS on the nonisothermal cold crystallization rate of PLLA was quantitatively evaluated by the following two methods. Based on a method suggested by Khanna,[38] a crystallization rate coefficient (CRC), representing a change in cooling rate required to bring about 1 °C change in the supercooling of the polymer melt, was introduced to compare the crystallization rate of different polymer systems. According to this method, the values of CRC were determined from the slope of the linear plot of cooling rate versus $T_m - T_p$, where T_m and T_p are the melting point and nonisothermal melt crystallization peak temperature, respectively. However, in the present work, the nonisothermal cold crystallization behavior of neat PLLA and its nanocomposites was studied from the amorphous state. Therefore, we modified the determination of CRC using $T_p - T_g$ instead of $T_m - T_p$, where T_p and T_g were the nonisothermal cold crystallization peak temperature and glass transition temperature, respectively, representing a change in heating rate required to bring about 1 °C change in the superheating of the polymer amorphous phase.[11,15] It is clear that the value of CRC should be higher for the sample with faster crystallization rate. Figure 3(a) shows the related plots of all the samples. The values of CRC are also summarized in Table I, from which tsib-POSS enhanced the nonisothermal cold crystallization process of PLLA in the nanocomposites. Moreover, the great increment of CRC values from PLLA/tsib-POSS0.5 to PLLA/tsib-POSS1, that is, from 0.535 to 0.739 min^{-1}, also manifested the fact that the change of tsib-POSS loading significantly influenced the cold crystallization rate of PLLA.

Another parameter, the crystallization rate parameter (CRP), was also used for the comparison of the crystallization rates of neat PLLA and its nanocomposites in this work. The CRP represents the crystallization rate of polymers, as was proposed by Zhang *et al.*[39–44] In the plots of $1/t_{1/2}$ versus heating rate, the CRP values could be obtained from the slopes of the straight lines, and a faster crystallization rate leaded to a higher slope. Figure 3(b) shows the related plots of all the samples, and the detailed CRP values are listed in Table I. The increased CRP values of the nanocomposites indicated again the efficiency of tsib-POSS in improving the cold crystallization rate of PLLA matrix. Meanwhile, the increment of tsib-POSS loading also slightly increased the CRP values, indicating that the increase of tsib-POSS loading may promote the nonisothermal cold crystallization rate of PLLA matrix.

As the CRC and CRP values quantitatively evaluate the effect of nanofiller on the nonisothermal cold crystallization rate of semicrystalline polymer matrix, they may also be used to compare the effect of different nanofillers on the nonisothermal cold crystallization behavior of the same polymer matrix. In previous work, we reported the CRC and CRP values of the PLLA/octavinyl-polyhedral oligomeric silsesquioxanes (ovi-POSS) nanocomposites, which were also nonisothermally crystallized from the amorphous state.[15] By comparing the CRC and CRP values, we found that the addition of 1 wt % ovi-

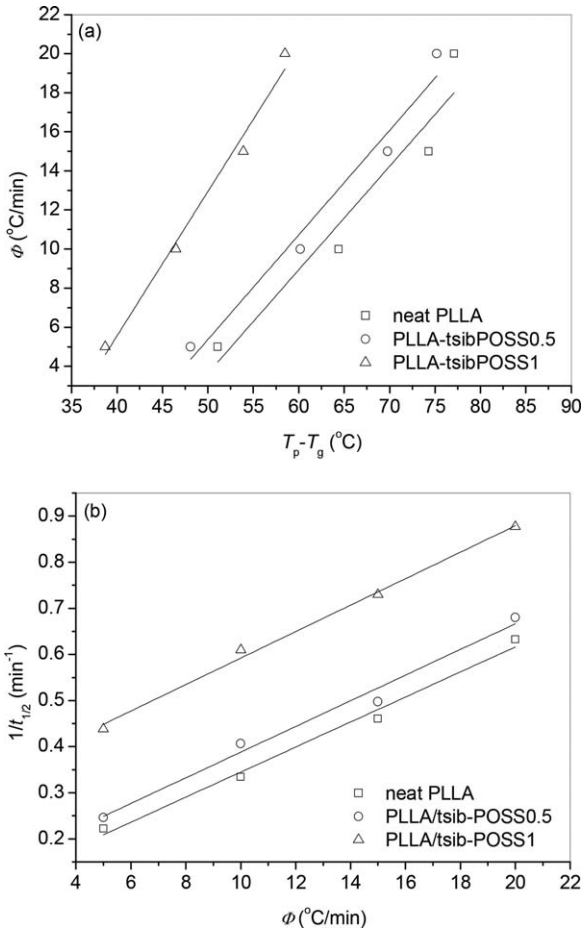

Figure 3. Effect of the tsib-POSS loading on the cold crystallization rate of PLLA: (a) crystallization rate coefficient and (b) crystallization rate parameter.

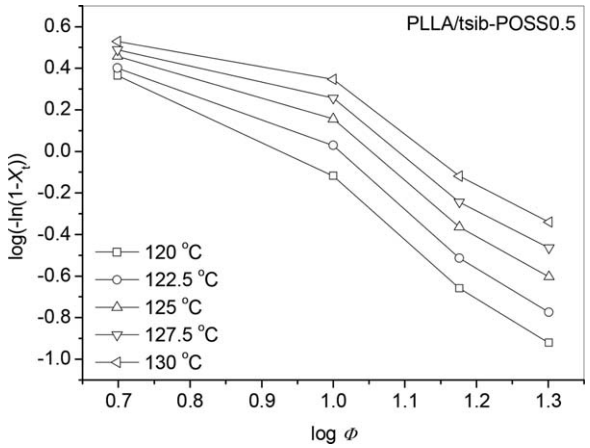

Figure 4. The Ozawa plots of PLLA/tsib-POSS0.5.

POSS caused a 53.8% increase in CRC and a 112.0% increase in CRP compared with those of neat PLLA; however, the addition of 1 wt % tsib-POSS only caused a 39.4% increase in CRC and a 5.5% increase in CRP compared with those of neat PLLA. Therefore, ovi-POSS enhanced the nonisothermal cold crystallization process of PLLA more efficiently than tsib-POSS.

Moreover, in previous work, the CRC and CRP values for neat PLLA were 0.302 min^{-1} and 0.0184 $°C^{-1}$, respectively.[15] The CRC and CRP values of neat PLLA in previous work were different from those in this work. The difference may be explained as follows. In previous work, the chosen heating rates were from 2.5 to 12.5 °C/min, while in the present work, the chosen heating rates were from 5 to 20 °C/min. As the CRC and CRP values were derived from the slopes of the linear fitting of the plots of Φ versus $T_p - T_g$ and the plots of $t_{1/2}$ versus Φ, respectively, different heating rate range may cause the differences of the CRC and CRP values.

To study the nonisothermal cold crystallization kinetics, several methods based on the Avrami equation have already been developed.[45–48] In this work, the nonisothermal cold crystallization kinetics of neat PLLA and its nanocomposites was first studied with the most well-known Ozawa model, which could be used when the crystallization behavior proceeded at a constant heating (or cooling) rate.[47] The Ozawa equation is written as follows:

$$X_t = 1 - \exp\left(\frac{-K(T)}{\Phi^m}\right) \quad (1)$$

where $K(T)$ is the heating (or cooling) function at crystallization temperature T, and m is the Ozawa exponent, which depends on the type of nucleation and growth mechanism.[47] Double logarithms of eq. (1) and rearrangement resulted in the following form:

$$\log[-\ln(1-X_t)] = \log K(T) - m \log \Phi \quad (2)$$

It should be noted that if the Ozawa equation fitted the crystallization of PLLA and its nanocomposites very well, there should be a series of parallel lines in the plots of $\log[-\ln(1 - X_t)]$ versus $\log \Phi$; thus, the parameters m and $K(T)$ could be obtained from the slopes and the intercepts, respectively.

The Ozawa plots of PLLA/tsib-POSS0.5 are shown in Figure 4 as an example, but the linearity of the lines was not obtained. Therefore, the Ozawa equation failed to fit the nonisothermal cold crystallization of PLLA, probably because the Ozawa equation neglected the strong secondary crystallization. Similar results were also found in some other composite systems.[11,15,43]

Although the Ozawa equation failed to fit the crystallization of PLLA, the theory proposed by Tobin was chosen in this work to study the nonisothermal cold crystallization kinetics of neat PLLA and its nanocomposites.[48] The Tobin equation is described as follows:

$$X_t = \frac{k_t t^{n_t}}{1 + k_t t^{n_t}} \quad (3)$$

where X_t is the relative crystallinity as a function of time, k_t is the Tobin crystallization rate constant, and n_t is the Tobin exponent. Based on this proposition, the Tobin exponent n_t does not need to be integral, since it is controlled directly by different types of nucleation and growth mechanism.[48] Equation (3) could be rewritten as follows to calculate the Tobin crystallization kinetics parameters:

$$\log[X_t/(1-X_t)] = \log k_t + n_t \log t \quad (4)$$

Figure 5 illustrates the Tobin plots of PLLA/tsib-POSS0.5 as an example, and the Tobin parameters n_t and k_t were obtained, respectively, from the slopes and intercepts of the fitted straight lines. The series of straight lines clearly indicated that the Tobin equation better described the nonisothermal cold crystallization process of PLLA than the Ozawa equation. Similar plots were obtained for other samples. For brevity, they were not shown here. The n_t values were around 4.46 for all the samples, indicating that the addition of tsib-POSS or the change of heating rates did not change the nonisothermal cold crystallization mechanism of PLLA. However, it should be noticed that at higher X_t range (larger than 75%), the experimental data were larger than the values concluded from the Tobin equation. The reason might be that the Tobin equation overemphasized the impingement effect, or because the model was too simplified to describe a rather more complicated process. In some other studies, similar results have also been found.[15,28,49]

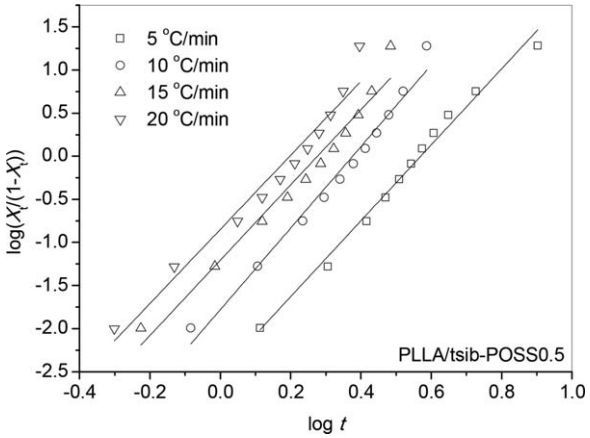

Figure 5. The Tobin plots of PLLA/tsib-POSS0.5.

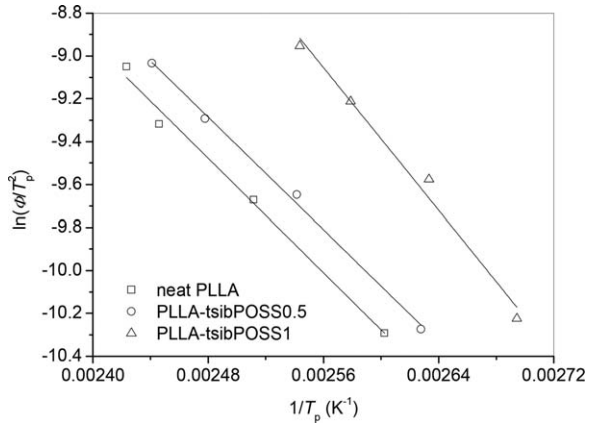

Figure 6. The Kissinger plots of neat PLLA and its nanocomposites for the estimation of crystallization activation energy in nonisothermal cold crystallization.

The activation energies for the nonisothermal cold crystallization of neat PLLA and PLLA/tsib-POSS nanocomposites were calculated from the Kissinger method,[50] which was written as follows:

$$\frac{d\left[\ln\left(\frac{\Phi}{T_p^2}\right)\right]}{d\left(\frac{1}{T_p}\right)} = -\frac{\Delta E}{R} \tag{5}$$

where ΔE is the activation energy, T_p is the crystallization peak temperature, and R is the universal gas constant. Figure 6 dispalys the Kissinger plots of neat PLLA and its nanocomposites. The ΔE values were estimated to be 55.4 ± 3.7, 54.5 ± 2.1, and 69.2 ± 5.6 kJ/mol for neat PLLA, PLLA/tsib-POSS0.5, and PLLA/tsib-POSS1, respectively. The ΔE value of PLLA/tsib-POSS0.5 was similar to that of neat PLLA, as the tsib-POSS content was only 0.5 wt %, while the ΔE value of PLLA/tsib-POSS1 was obviously increased. Because tsib-POSS lowered the nonisothermal cold crystallization peak temperatures for the nanocomposites, the movement of PLLA chain segments to the growing surface was restrained, thereby causing the increase in ΔE. This phenomenon was also found in other PLLA-based nanocomposites, such as PLLA/ovi-POSS, PLLA/MWCNTs, and PLLA/clay nanocomposites.[11,15,31]

Isothermal Cold Crystallization Kinetics of Neat PLLA and its Nanocomposites

Figure 7 shows the evolution of heat flow with crystallization time, plots of relative crystallinity versus crystallization time, and the related Avrami plots for PLLA/tsib-POSS0.5 crystallized at indicated T_c values as an example. As shown in Figure 7(a,b), at a higher T_c, the time to finish crystallization became shorter, indicating that the crystallization process of PLLA was accelerated. Similar plots were obtained for other samples and are not shown here for brevity.

The isothermal cold crystallization kinetics of neat PLLA and its nanocomposites was analyzed by the famous Avrami equation as follows:

$$1 - X_t = \exp(-kt^n) \tag{6}$$

where k and n are the Avrami parameters, which reflect the crystallization rate and crystallization mechanism, respectively.[51,52]

The related Avrami plots of PLLA/tsib-POSS0.5 are illustrated in Figure 7(c) as an example, and all the n and k data are summarized in Table II. For all the samples isothermally crystallized at different T_c values, the n values were around 2.3, indicating that the isothermal cold crystallization mechanism of PLLA remained unchanged despite the change of T_c values or the introduction of tsib-POSS.

As the unit of k (min^{-n}) had different n values at indicated T_c values, it was not reasonable to discuss the crystallization rate

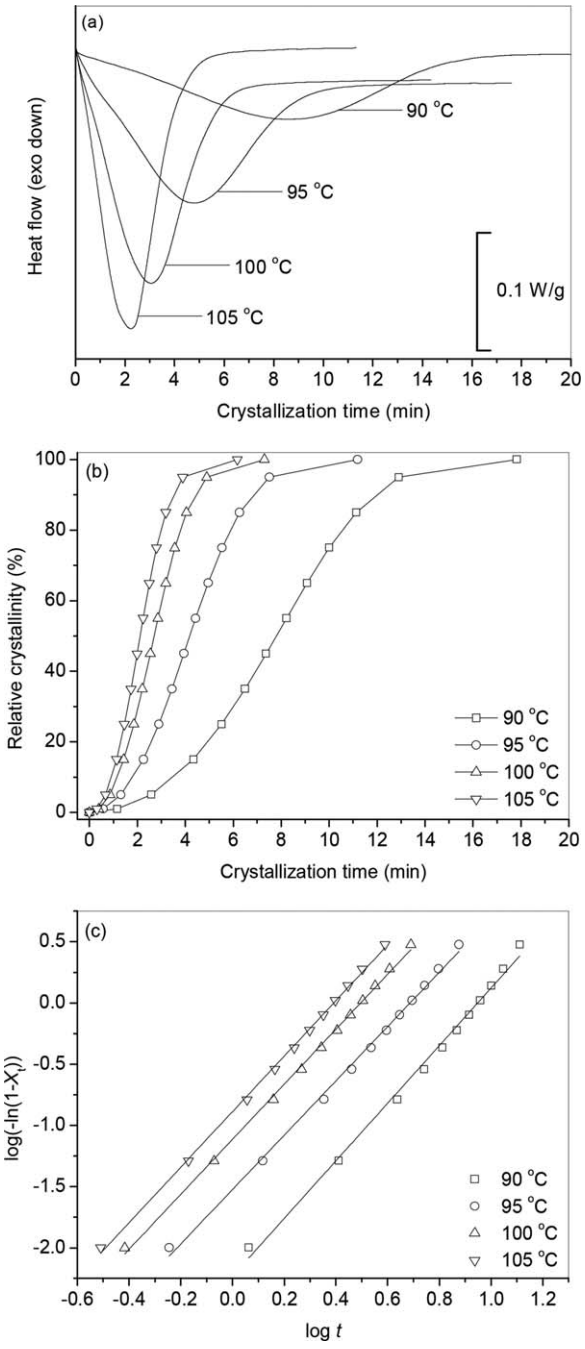

Figure 7. (a) Evolution of heat flow with crystallization time, (b) plots of relative crystallinity versus crystallization time, and (c) the related Avrami plots for PLLA/tsib-POSS0.5 crystallized at indicated T_c values.

Table II. Summary of the Isothermal Cold Crystallization Kinetics Parameters Based on the Avrami Equation for Neat PLLA and its Nanocomposites at Indicated T_c Values

Samples	T_c (°C)	ΔH_c[a] (J/g)	n	k (min^{-n})	$t_{0.5}$ (min)
Neat PLLA	90	22.5	2.3	2.1×10^{-3}	12.4
	95	31.4	2.2	1.2×10^{-2}	6.4
	100	32.2	2.2	3.8×10^{-2}	3.8
	105	35.5	2.2	7.6×10^{-2}	2.7
PLLA/tsib-POSS0.5	90	26.9	2.4	5.9×10^{-3}	7.3
	95	28.8	2.2	3.0×10^{-2}	4.2
	100	32.4	2.2	7.7×10^{-2}	2.7
	105	36.7	2.3	1.3×10^{-1}	2.1
PLLA/tsib-POSS1	90	27.2	2.2	4.6×10^{-2}	3.4
	95	30.4	2.2	2.0×10^{-1}	1.8
	100	32.7	2.3	5.3×10^{-1}	1.1
	105	35.7	2.2	1.1	0.8

[a] The error is within ±1 J/g.

by comparing the k values directly. Thus, the crystallization half-time ($t_{0.5}$) was employed to compare the crystallization rate. The values of $t_{0.5}$ were calculated by the following equation and are listed in Table II:

$$t_{0.5} = \left(\frac{\ln 2}{k}\right)^{1/n} \quad (7)$$

As a greater $t_{0.5}$ corresponded to a slower crystallization rate, it was more obvious to compare the influences of T_c and the tsib-POSS loading on the crystallization rate from the plots of $1/t_{0.5}$ versus T_c.

Figure 8 shows the plots of $1/t_{0.5}$ versus T_c. For all the samples, $1/t_{0.5}$ increased with increasing T_c; moreover, when the loading of tsib-POSS increased from 0.5 to 1 wt %, $1/t_{0.5}$ of the nanocomposites obviously increased at the same T_c, indicating that the increment of tsib-POSS loading had a more distinct influence on the crystallization rate of PLLA. In conclusion, the addition of tsib-POSS could enhance both the nonisothermal and isothermal cold crystallization kinetics of PLLA matrix in the nanocomposite.

Crystal Structure of Neat PLLA and its Nanocomposites

The WAXD patterns for neat PLLA and its nanocomposites after isothermal cold crystallization at 90 °C are shown in Figure 9. It could be distinctly seen from Figure 9 that neat PLLA exhibited two sharp characteristic diffraction peaks at $2\theta = 16.5°$ and 18.9°, corresponding to (200)/(110) and (203) planes, respectively.[34] Besides, a small peak located at $2\theta = 24.7°$ was also noticed in Figure 9, which was characteristic for the α′-form of PLLA,[35,37] indicating the formation of α′-form during the isothermal cold crystallization process of PLLA at 90 °C. Similar diffraction peaks also existed for the nanocomposites, confirming that the crystal structure of PLLA remained unchanged in the nanocomposites. In brief, tsib-POSS did not modify the crystal structure of PLLA.

In addition, as shown in Figure 9, neat tsib-POSS was highly crystalline. However, the characteristic diffraction peaks of tsib-

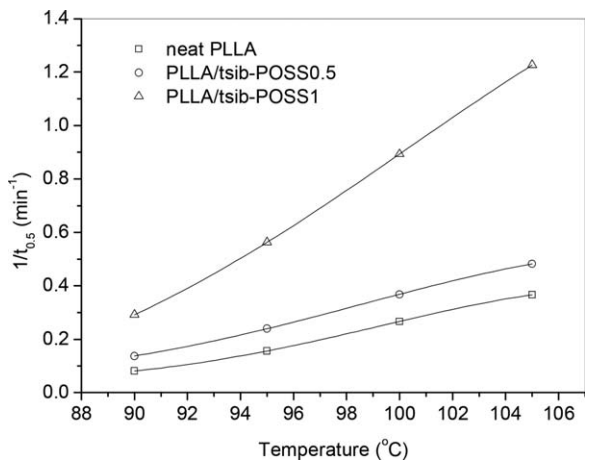

Figure 8. Plots of $1/t_{0.5}$ with T_c for neat PLLA and its nanocomposites.

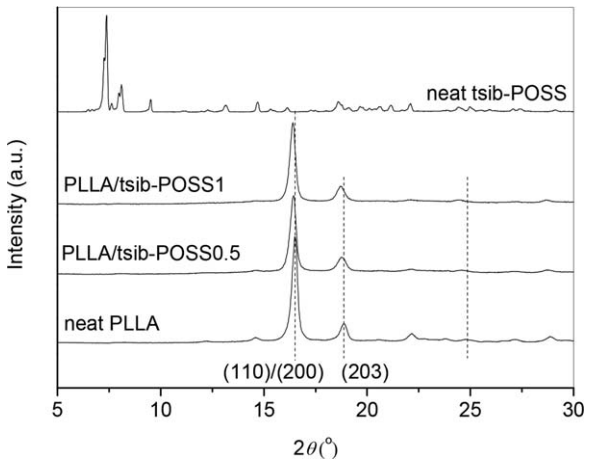

Figure 9. WAXD patterns for neat PLLA and its nanocomposites after isothermal cold crystallization at 90 °C.

POSS did not appear in the PLLA/tsib-POSS nanocomposites, for the contents of tsib-POSS were only 0.5 and 1 wt %. In the PLLA/tsib-POSS nanocomposites, the highly crystalline tsib-POSS may exist as crystals during the cold crystallization process of PLLA, thereby providing a number of sites for PLLA to nucleate. Moreover, the hydroxyl group of tsib-POSS may show some interactions with the carbonyl group of PLLA matrix. Thus, tsib-POSS showed an efficient nucleating agent effect in the PLLA matrix.

CONCLUSIONS

In this work, neat PLLA and its nanocomposites at low tsib-POSS loadings were prepared via a solution and casting method; furthermore, the cold crystallization kinetics and crystal structure of all the samples were fully investigated. Different heating rates were chosen to investigate the nonisothermal cold crystallization process of neat PLLA and its nanocomposites. The results indicated that the change of both heating rate and the tsib-POSS loading may have great influences on the nonisothermal cold crystallization behavior of neat PLLA and its nanocomposites. For all the samples, with the increase of heating rate, the crystallization exotherms became broader, and the cold crystallization peak temperature shifted upward. Meanwhile, at a chosen heating rate, tsib-POSS increased the nonisothermal crystallization rate of PLLA. Moreover, the increment of tsib-POSS loading obviously enhanced the crystallization rate of PLLA, as was proved by the calculation of crystallization rate coefficient and crystallization rate parameter. For the nonisothermal cold crystallization kinetics study, the Ozawa and Tobin equation were both used to describe the crystallization process of the samples, and the Tobin equation fitted it better. The nonisothermal cold crystallization activation energy was calculated by the Kissinger method, which was larger for PLLA/tsib-POSS1 than for neat PLLA. For the isothermal cold crystallization kinetics study, when the samples were crystallized at the same crystallization temperature, the addition of tsib-POSS and the increment of tsib-POSS loading could increase the crystallization rate of PLLA, showing an efficient nucleation agent effect of tsib-POSS. However, the crystallization mechanism and crystal structure of PLLA were not modified by tsib-POSS in the nanocomposites.

ACKNOWLEDGMENTS

Part of this research was financially supported by the National Natural Science Foundation, China (51373020, 51573016, and 51521062).

REFERENCES

1. Madhavan Nampoothiri, K.; Nair, N. R.; John, R. P. *Bioresour. Technol.* **2010**, *101*, 8493.
2. Auras, R.; Harte, B.; Selke, S. *Macromol. Biosci.* **2004**, *4*, 835.
3. Ikada, Y.; Tsuji, H. *Macromol. Rapid Commun.* **2000**, *21*, 117.
4. Raquez, J. M.; Habibi, Y.; Murariu, M.; Dubois, P. *Prog. Polym. Sci.* **2013**, *38*, 1504.
5. Sinha Ray, S.; Maiti, P.; Okamoto, M.; Yamada, K.; Ueda, K. *Macromolecules* **2002**, *35*, 3104.
6. Maiti, P.; Yamada, K.; Okamoto, M.; Ueda, K.; Okamoto, K. *Chem. Mater.* **2002**, *14*, 4654.
7. Paul, M. A.; Alexandre, M.; Degée, P.; Henrist, C.; Rulmont, A.; Dubois, P. *Polymer* **2003**, *44*, 443.
8. Huang, H. D.; Ren, P. G.; Xu, J. Z.; Xu, L.; Zhong, G. J.; Hsiao, B. S.; Li, Z. M. *J. Membr. Sci.* **2014**, *464*, 110.
9. Wang, H.; Qiu, Z. *Thermochim. Acta* **2011**, *526*, 229.
10. Zhao, Y.; Qiu, Z.; Yang, W. *J. Phys. Chem. B* **2008**, *112*, 16461.
11. Zhao, Y.; Qiu, Z.; Yan, S.; Yang, W. *Polym. Eng. Sci.* **2011**, *51*, 1564.
12. Yu, J.; Qiu, Z. *ACS Appl. Mater. Interfaces* **2011**, *3*, 890.
13. Qiu, Z.; Pan, H. *Compos. Sci. Technol.* **2010**, *70*, 1089.
14. Pan, H.; Qiu, Z. *Macromolecules* **2010**, *43*, 1499.
15. Yu, J.; Qiu, Z. *Ind. Eng. Chem. Res.* **2011**, *50*, 12579.
16. Yu, J.; Qiu, Z. *Thermochim. Acta* **2011**, *519*, 90.
17. Cordes, D. B.; Lickiss, P. D.; Rataboul, F. *Chem. Rev.* **2010**, *110*, 2081.
18. Wu, J.; Mather, P. T. *Polym. Rev.* **2009**, *49*, 25.
19. Kannan, R. Y.; Salacinski, H. J.; Butler, P. E.; Seifalian, A. M. *Acc. Chem. Res.* **2005**, *38*, 879.
20. Kuo, S. W.; Chang, F. C. *Prog. Polym. Sci.* **2011**, *36*, 1649.
21. Fina, A.; Monticelli, O.; Camino, G. *J. Mater. Chem.* **2010**, *20*, 9297.
22. Deng, J.; Polidan, J. T.; Hottle, J. R.; Farmer-Creely, C. E.; Viers, B. D.; Esker, A. R. *J. Am. Chem. Soc.* **2002**, *124*, 15194.
23. Deng, J.; Hottle, J. R.; Polidan, J. T.; Kim, H. J.; Farmer-Creely, C. E.; Viers, B. D.; Esker, A. R. *Langmuir* **2004**, *20*, 109.
24. Kim, H. J.; Deng, J.; Lalli, J. H.; Riffle, J. S.; Viers, B. D.; Esker, A. R. *Langmuir* **2005**, *21*, 1908.
25. Liu, Y. R.; Huang, Y. D.; Liu, L. *Polym. Degrad. Stabil.* **2006**, *9*, 2731.
26. Liu, Y. R.; Huang, Y. D.; Liu, L. *Compos. Sci. Technol.* **2007**, *67*, 2864.
27. Ciolacu, F. C. L.; Choudhury, N. R.; Dutta, N.; Kosior, E. *Macromolecules* **2007**, *40*, 265.
28. Tang, L.; Qiu, Z. *J. Nanosci. Nanotechnol.* Accepted for publication.
29. Qiu, Z.; Ikehara, T.; Nishi, T. *Polymer* **2003**, *44*, 5429.
30. Liao, R.; Yang, B.; Yu, W.; Zhou, C. *J. Appl. Polym. Sci.* **2007**, *104*, 310.
31. Wu, D.; Wu, L.; Wu, L.; Xu, B.; Zhang, Y.; Zhang, M. *J. Polym. Sci. B Polym. Phys.* **2007**, *45*, 742.
32. Saeidlou, S.; Huneault, M. A.; Li, H.; Park, C. B. *Prog. Polym. Sci.* **2012**, *37*, 1657.
33. Zhang, J.; Tashiro, K.; Domb, A. J.; Tsuji, H. *Macromol. Symp.* **2006**, *242*, 274.
34. Kawai, T.; Rahman, N.; Matsuba, G.; Nishida, K.; Kanaya, T.; Nakano, M.; Okamoto, H.; Kawada, J.; Usuki, A.;

Honma, N.; Nakajima, K.; Matsuda, M. *Macromolecules* **2007**, *40*, 9463.

35. Pan, P.; Zhu, B.; Kai, W.; Dong, T.; Inoue, Y. *J. Appl. Polym. Sci.* **2008**, *107*, 54.
36. Zhang, J.; Duan, Y.; Sato, H.; Tsuji, H.; Noda, I.; Yan, S.; Ozaki, Y. *Macromolecules* **2005**, *38*, 8012.
37. Zhang, J.; Tashiro, K.; Tsuji, H.; Domb, A. J. *Macromolecules* **2008**, *41*, 1352.
38. Khanna, Y. P. *Polym. Eng. Sci.* **1990**, *30*, 1615.
39. Zhang, R.; Zheng, H.; Lou, X.; Ma, D. *J. Appl. Polym. Sci.* **1994**, *51*, 51.
40. Supaphol, P.; Dangseeyun, N.; Srimoaon, P. *Polym. Test.* **2004**, *23*, 175.
41. Huang, J. W.; Hung, H. C.; Tseng, K. S.; Kang, C. C. *J. Appl. Polym. Sci.* **2006**, *100*, 1335.
42. Wu, M.; Yang, G.; Wang, M.; Wang, W.; Zhang, W. D.; Feng, J.; Liu, T. *Mater. Chem. Phys.* **2008**, *109*, 547.
43. Zhao, H.; Bian, Y.; Li, Y.; Han, C.; Dong, Q.; Dong, L.; Gao, Y. *Thermochim. Acta* **2014**, *588*, 47.
44. Yang, Z.; Peng, H.; Wang, W.; Liu, T. *J. Appl. Polym. Sci.* **2010**, *116*, 2658.
45. Jeziorny, A. *Polymer* **1978**, *19*, 1142.
46. Liu, T.; Mo, Z.; Wang, S.; Zhang, H. *Polym. Eng. Sci.* **1997**, *37*, 568.
47. Ozawa, T. *Polymer* **1971**, *12*, 150.
48. Tobin, M. C. *J. Polym. Sci. B: Polym. Phys.* **1974**, *12*, 399.
49. Li, Y.; Han, C. *Ind. Eng. Chem. Res.* **2012**, *51*, 15927.
50. Kissinger, H. *J. Res. Natl. Bur. Stand (U.S.)* **1956**, *57*, 217.
51. Avrami, M. *J. Chem. Phys.* **1940**, *8*, 212.
52. Avrami, M. *J. Chem. Phys.* **1941**, *9*, 177.